

ACCELERATION OF TRANSONIC POTENTIAL FLOW CALCULATIONS ON ARBITRARY MESHES BY THE MULTIPLE GRID METHOD*

Antony Jameson
Courant Institute of Mathematical Sciences, New York University, 251 Mercer Street
New York, New York 10012

Abstract

The paper describes a multiple grid method for transonic flow calculations. The proposed scheme incorporates a generalized alternating direction method as the smoothing algorithm. Numerical experiments with this multigrid alternating direction (MAD) method indicate that it is both fast and reliable.

1. Introduction

The multiple grid method was first proposed by Federenko [1], who realized that it should be possible to accelerate an iterative scheme for solving difference equations by calculating corrections for the fine grid equations on a sequence of successively coarser grids. This idea was subsequently analyzed by Bakhavlov [2], and then extended and applied to a variety of problems by Bradt [3]. It has recently been proved under rather general assumptions by Nicolaides [4], and Haxbush [5], that the number of operations required to solve the equations arising from a finite element or a finite difference approximation to an elliptic problem by a multiple grid method is directly proportional to the number of unknowns.

There is less experience of the use of multiple grid methods for nonelliptic problems. The first demonstration of the use of a multiple grid method for a transonic flow problem was by South and Brandt [6], who solved the transonic small disturbance equation for a nonlifting flow and observed a high rate of convergence. Difficulties were experienced, however, both by South and Brandt and by the present author, in the treatment of lifting flow and in calculations on nonuniform and curvilinear meshes. There was a tendency to produce an oscillating sonic line, and for the calculations to enter a variety of limit cycles between several grids. These difficulties appeared to be due to insufficient smoothing of the errors on fine grids before passing to coarser grids, and South and Brandt were able to obtain convergence for a wider range of cases by using multiple line relaxation sweeps in different directions. [7]

* This work was supported by the office of Naval Research under Contract N00014-77-C-0032 and by NASA under Grants NSG-1579 and NGR-33-016-201. The calculations were performed at the DOE Mathematics and Computing Laboratory under Contract EY-76-C-02-3077.

In the present work the difficulties have been attacked by combining the multiple grid method with a generalized alternating direction method suitable for transonic flows as the smoothing algorithm. Numerical experiments indicate that this multigrid alternating direction (MAD) method converges rapidly and reliably for a range of cases typical of the cruising regime, up to the onset of drag rise. It appears also that the method can readily be generalized to treat three-dimensional flows.

2. The Difference Approximation

The case which will be considered is that of two dimensional transonic flow past an airfoil using the potential flow approximation, which has been found to give useful predictions in practice for flow containing shock waves of moderate strength [8]. This potential flow equation will be treated in the conservation form.

$$\frac{\partial}{\partial x}(\rho u) + \frac{\partial}{\partial y}(\rho v) = 0 \quad (1)$$

where x and y are Cartesian coordinates, ρ is the density and the velocity components u and v are the gradient of the potential ϕ ,

$$u = \phi_x, \quad v = \phi_y. \quad (2)$$

If q is the speed $\sqrt{u^2 + v^2}$, the local speed of sound a is determined by Bernoulli's equation.

$$a^2 = a_0^2 - \frac{\gamma - 1}{2} q^2 \quad (3)$$

where a_0 is the stagnation speed of sound. The density follows from the relation

$$\rho^{\gamma-1} = M_\infty^2 a^2 \quad (4)$$

where M_∞ is the Mach number q/a of the uniform flow at infinity and γ is the ratio of specific heats. At the profile the potential satisfies the Neumann boundary conditions.

$$\frac{\partial \phi}{\partial n} = 0 \quad (5)$$

where n is the normal direction and also the Kutta condition that the tangential velocity is bounded at the trailing edge. At infinity, the potential approaches the potential of a vortex in compressible flow.

In the numerical experiments reported here these equations are solved in a coordinate system generated by a conformal mapping of the domain onto the interior of a circle. Using polar coordinates r and θ the potential flow equation becomes.

$$\frac{\partial}{\partial \theta} (\rho \phi_\theta) + r \frac{\partial}{\partial r} (r \rho \phi_r) = 0 \quad (6)$$

The velocity components in the θ and r directions are

$$u = \frac{r \phi_\theta}{H}, \quad v = \frac{r^2 \phi_r}{H} \quad (7)$$

where H is the modulus of the transformation onto the exterior of the circle.

The difference approximation is similar to schemes which have been previously used [8]. It is derived by augmenting a central difference scheme with an artificial viscosity which introduces an upwind bias throughout the supersonic zone. Using sub-scripts i, j to denote values at mesh points, and $i+1/2, j+1/2$ to denote values at the midpoints of the segments connecting mesh points, the approximation to equation [6] has the form

$$\begin{aligned} & \frac{1}{\Delta \theta^2} \left\{ \rho_{i+1/2, j} (\phi_{i+1, j} - \phi_{i, j}) \right\} \\ & - \rho_{i-1/2, j} (\phi_{i, j} - \phi_{i-1, j}) \\ & + \frac{r_j}{\Delta r^2} \left\{ r_{j+1/2} \rho_{i, j+1/2} (\phi_{i, j+1} - \phi_{i, j}) \right. \\ & \left. - r_{j-1/2} \rho_{i, j-1/2} (\phi_{i, j} - \phi_{i, j-1}) \right\} + T_{ij} = 0 \quad (8) \end{aligned}$$

where $\Delta \theta$ and Δr are the mesh widths, and T_{ij} is the artificial viscosity. The flow in the supersonic zone is assumed to be roughly in the θ direction and a artificial viscosity which gives a bias only in the θ direction has been used in the experiments so far. Let μ be a switching function

$$\mu = \max \left\{ 0, \left(1 - M_c^2 / M^2 \right) \right\} \quad (9)$$

which vanishes when the local Mach number M is below a cutoff Mach number M_c , and let $S_{i,j}$ be a difference approximation to $\mu \rho (u^2/a^2) \phi_{\theta\theta}$ at the point i, j . Then the artificial viscosity is of the form

$$T_{i,j} = P_{i+1/2,j} - P_{i-1/2,j} \quad (10)$$

where

$$P_{i+1/2,j} = \begin{cases} S_{i,j} - \varepsilon S_{i-1,j} & \text{if } u_{i+1/2,j} > 0 \\ S_{i+1,j} - \varepsilon S_{i+2,j} & \text{if } u_{i+1/2,j} < 0 \end{cases} \quad (11)$$

and ε is a parameter controlling the accuracy. If $\varepsilon = 0$ the added terms are of order $\Delta \theta$, yielding a first order accurate scheme, and if $\varepsilon = 1$ the added terms are of order $\Delta \theta^2$, yielding a second order accurate scheme. This cutoff value $M_c^2 = 0.9$ has been found to result in reliable convergence of the multigrid alternating direction scheme.

3. Review of the Multiple Grid Method

Consider the solution of the equation

$$L^h u = f \quad (12)$$

by a relaxation method, where L^h approximates a linear differential operator L on a grid with a spacing proportional to the parameter h . let U be an approximation to the solution, and let V be the correction to U such that $U + V$ satisfies, (12). Then the basis of the multiple grid method is to replace (12) by

$$L^{2h} v + I_h^{2h} L^h U = f \quad (13)$$

where L^{2h} is the same approximation to L on a grid in which the spacing has been doubled, and I_h^{2h} is an operator which transfers to each grid point of the coarse grid the residual $L^h U - f$ of the coincident point of the fine mesh, or alternatively a weighted average of the residuals at neighboring points. After solution of (13), the approximation on the fine grid is updated by interpolating the correction calculated on the coarse grid to the fine grid, so that U is replaced by

$$U^{new} = U + I_{2h}^h V \quad (14)$$

where I_{2h}^h is an interpolation operator. Equation (13) can in turn be solved by introducing an approximation on a yet coarser grid, so that a multiple sequence of grids may be used, leading to a rapid solution procedure for two reasons. First, the number of operations required for a relaxation sweep on one of the coarse grids is much smaller than the number required on the fine grid. Second, the rate of convergence is faster on a coarse grid, reflecting the fact that corrections can be propagated from one end of the grid to the other in a small number of steps.

To extend this idea to non linear equations, equation (13) may be reorganized by adding and subtracting the current solution U to give

$$L^{2h}(U + V) + I_h^{2h} L^h U - L^{2h} U = f$$

or

$$L^{2h} \bar{U} = \bar{f} \quad (15)$$

where \bar{U} is the improved estimate of the solution to be determined on the coarse grid, and \bar{f} is an appropriately modified right-hand side,

$$\bar{f} = f + L^{2h} U - I_h^{2h} L^h U \quad (16)$$

The updating formula (14) now becomes

$$U^{new} = U + I_h^h (\bar{U} - U) \quad (17)$$

This avoids the need to introduce a special perturbation operator to represent the correction equation (13).

4. Smoothing Algorithms

The success of the multiple grid method generally depends on the use of a relaxation algorithm which rapidly reduces the high frequency components of error on any given grid, because on a coarser grid these components can not be distinguished from low frequency components. This aliasing process will cause improper corrections to be computed on coarse grids, and can prevent convergence.

It turns out that point and line relaxation schemes do not necessarily provide the required smoothing of all high frequency components of error on a non uniform or curvilinear mesh. To illustrate this consider the model problem

$$a\phi_{xx} + b\phi_{yy} = 0 \quad (18)$$

with positive coefficients $a > 0$, $b > 0$. Let δ_x^2 and δ_y^2 denote second difference operator in the x and y directions, and suppose that the difference approximation has the form

$$L\phi = (A\delta_x^2 + B\delta_y^2)\phi = 0 \quad (19)$$

where if Δx and Δy are the mesh widths,

$$A = \frac{a}{\Delta x^2}, \quad B = \frac{b}{\Delta y^2} \quad (20)$$

Assuming periodic boundary conditions suppose that the solution after n iterations has the form

$$\phi = G^n e^{ipx} e^{iqy} \quad (21)$$

where G is the amplification factor, and let

$$p\Delta x = \xi, \quad q\Delta y = \eta$$

Then a Gauss Seidel scheme yields

$$G = \frac{Ae^{i\xi} + Be^{i\eta}}{A(2 - e^{-i\xi}) + B(2 - e^{-i\eta})}$$

Suppose that Δx , Δy are such that $A \gg B$ and consider the case of a high frequency in the y direction and a low frequency in the x direction, which may be represented by $\xi = 0$, $\eta = \pi$. Then

$$G = \frac{A - B}{A + 3B} \sim 1$$

A similar analysis of a line relaxation scheme shows that if $A \gg B$ effective damping of high frequency error components requires the use of a scheme solving along the lines in the x direction [6].

On a nonuniform grid A and B may vary widely so that in some regions $A \gg B$ and in others $B \gg A$. This has led South and Brandt to use multiple line relaxations sweeps in different directions [7]. An alternative approach proposed by Arlinger [9] is to use auxiliary grid constructed by increasing the mesh width in one direction only while the line relaxation scheme is applied to the lines in the other direction. This method has been tested by the present writer and found to give a useful acceleration of the rate of convergence of transonic flow calculations, its potential efficiency, however, in less than that of a full multigrid scheme in which the mesh width is increased in both directions, because the coarse grids contain more mesh points when the mesh width is only increased in one direction.

It is proposed here to use an alternating direction method as the smoothing algorithm. Consider the model equation (18) and suppose that the correction $\delta\phi$ is calculated by the equation

$$(\alpha - A\delta_x^2)(\alpha - B\delta_y^2)\delta\phi = \omega\alpha L\phi \quad (22)$$

where α is a parameter to be chosen, ω is an overrelaxation factor, and the residual $L\phi$ is calculated using the result of the previous iteration. (The usual Peaceman-Rechford scheme [10] is obtained by setting $\omega = 2$). Then on inserting a trial solution of the form [21] it is found that all high frequency components are rapidly damped if

$$\alpha \sim 4 \min(A, B), \quad \omega \sim 1.5$$

(assuming that $A > 0$, $B > 0$).

5. Generalized Alternating Direction Scheme

In the case of transonic flow we have to allow for a change from elliptic to hyperbolic type as the flow becomes locally supersonic. In the model

problem (18) this corresponds to one of the coefficients, a say, becoming negative. The classical alternating direction scheme (22) then has the disadvantage that if one regards the iterations as representing time steps Δt in an artificial time direction t [11], it simulates the time dependent equation

$$\alpha \Delta t \phi_t = a \phi_{xx} + b \phi_{yy}$$

When $a < 0$ and Cauchy data is given at $x = 0$, corresponding to supersonic inflow, this leads to an ill posed problem which admits oscillatory solutions which are undamped in time and grow in the x direction.

The following generalized alternating direction scheme is therefore proposed. Let the scalar parameter α in equation (22) be replaced by a difference by a difference operator

$$S \equiv \alpha_0 + \alpha_1 \delta_x^- + \alpha_2 \delta_y^- \quad (23)$$

Where δ_x^- and δ_y^- denote one sided difference operators in the x and y directions. This yields the scheme

$$(S - A \delta_x^2)(S - B \delta_y^2) \delta \phi = \omega S L \phi \quad (24)$$

in which the residual $L\phi$ is differenced by the operator S . The corresponding time dependant equation is now a hyperbolic equation of the form

$$\beta_0 \phi_t + \beta_1 \phi_{xt} + \beta_2 \phi_{yt} = a \phi_{xx} + b \phi_{yy}$$

where the coefficients, $\beta_0, \beta_1, \beta_2$ depend on the parameters $\alpha_0, \alpha_1, \alpha_2$.

The artificial viscosity introduced in Section 2 is equivalent to a switch to upwind differencing in the x direction as was first proposed by Murman and Cole [12], and in the implementation of the scheme the difference operator δ_x^2 in the first factor is correspondingly replaced by an unwind difference operator when $A < 0$, and the direction of the one sided operator δ_x^- in S is chosen to be upwind.

The generalized scheme (24) can be related to previously proposed alternating direction methods for transonic flows [13, 14] by appropriate specialization of the parameters. For example, the AF2 scheme proposed by Ballhaus, Jameson and Albert [13], corresponds to the choice $\alpha_0 = 0, \alpha_2 = 0$, followed by integration in the x direction which eliminates the differencing of the residual.

6. Multiple Grid Strategy

Theoretical estimates of the rate of convergence attainable by the use of multiple grids have been obtained for recursive strategies [4, 5]. South and Brandt [6] used an adaptive strategy, with transitions to a coarser grid if the rate of convergence becomes too low on a particular grid, or to a finer grid if the average residual has been sufficiently reduced.

In the present work a simple fixed strategy has been found to be effective. Each cycle begins on the fine grid. The alternating direction iteration is performed once on each grid until the coarsest grid is reached. Then it is performed once on each grid going back up to the second finest grid, and the cycle terminates with the interpolation of the correction from the second finest, grid to the fine grid. It is convenient to measure the work in units representing the work required to perform one iteration of the alternating direction scheme on the fine grid. Since each grid has 1/4 as many cells as the next finer grid, the work required to perform each cycle is

$$1 + 2 \left[\frac{1}{4} + \frac{1}{16} + \frac{1}{64} \dots \right] \leq 1 \frac{2}{3} \text{ units,}$$

plus the overhead of computing and transmitting residuals from one grid to the next, and interpolating the corrections.

It is the usual practice to accelerate the alternating direction scheme (22) by using a sequence of values of the parameter α designed to give rapid damping of the error components in a series of frequency bands. The multigrid alternating direction method economizes the work required by passing to the coarse grids to treat the error components in the low frequency bands. If a sequence of 6 parameters were used to treat 6 frequency bands, for example, the work required to complete one cycle through the parameters would be 6 units, whereas the work required to perform the alternating direction iterations of a multigrid cycle with 6 grids would be less than $1 \frac{2}{3}$ units with the present strategy.

7. Results

The efficiency of the multigrid alternating direction method has been confirmed by numerical experiments. Some typical results are presented here. All the examples were calculated on a circular domain generated by conformal mapping of the profile to a unit circle, with 192 cells in the θ and 32 cells in the r direction on the fine grid. Up to 6

grids were used, giving a coarse grid with as few as 6 cells in the θ direction and 1 cell in the r direction.

Figure 1 shows the observed convergence rate using different numbers of grids for a case with a shock of moderate strength, the flow past an NACA 64A410 airfoil at Mach 0.720 and an angle of attack of 0° . The pressure distribution of the fully converged result is shown in Figure 1a. Figures 1b-1g show the logarithm of the average absolute value of the residual plotted against the work, measured by the equivalent number of iterations on the fine grid. The convergence rate, measured as the mean reduction in the average residual per unit of work, is also indicated under each graph. It can be seen that the rate of convergence was improved from 0.9840 to 0.6677 as the number of grids was increased from 1 to 5, while no further improvement was realized with 6 grids. (In subsonic flow it pays to use 6 grids).

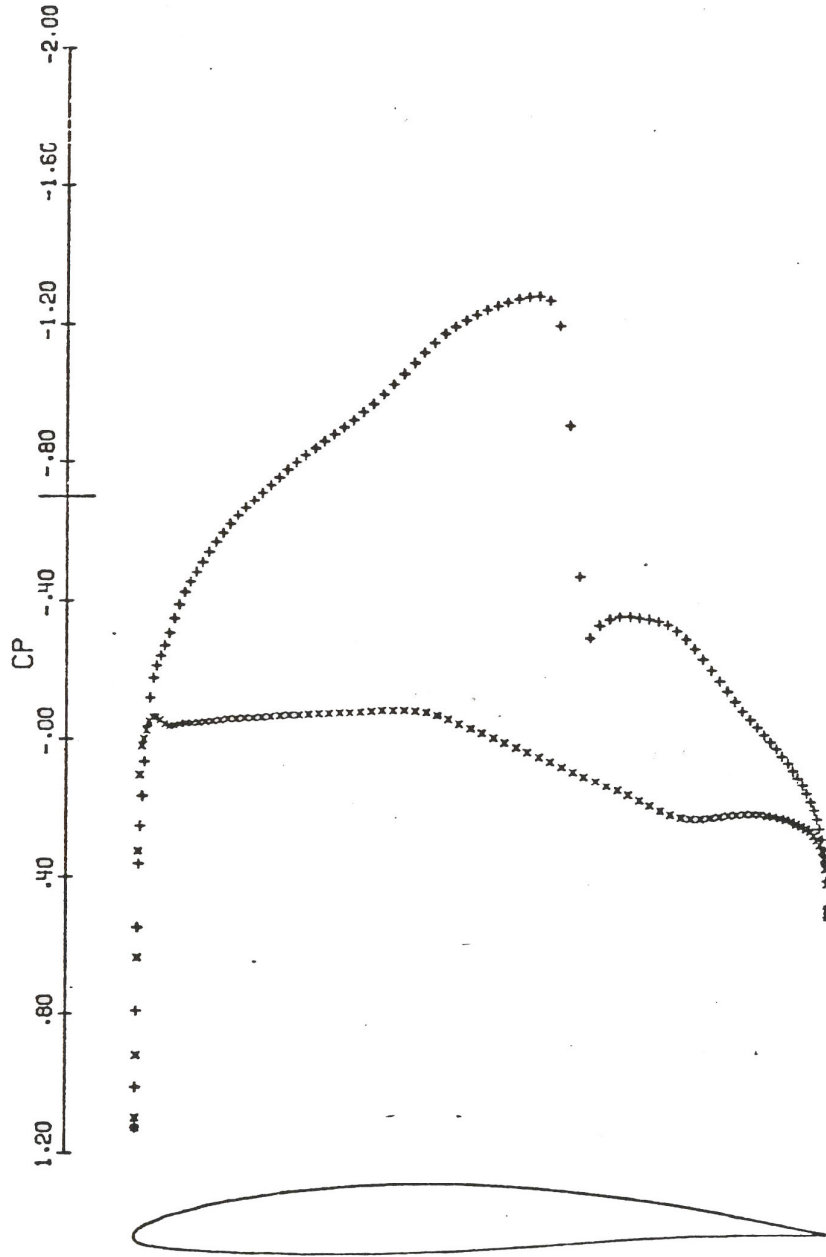
Figure 2 shows a case with a fairly strong shock, the flow past an NACA 0012 airfoil at Mach 0.750 and an angle of attack of 2° . In this case the calculation converges rapidly after an initial hesitation. A study of plots of the pressure distribution after each cycle shows that the formation of the shock is accompanied by the appearance ahead of the shock of a temporary overshoot which is subsequently suppressed. The first order accurate scheme obtained by setting $\varepsilon=1$ in equation (11) was used both in this calculation and in the calculations displayed in Figure 1.

Figure 3 shows the initial convergence history of the calculation of a flow containing two shocks, to illustrate the speed with which the flow pattern is established. The case is that of a Korn airfoil at a Mach number slightly below its design point, calculated with the second order accurate scheme obtained by setting $\varepsilon = 1$ in equation [11]. (The forward shock was suppressed when the calculation was repeated with $\varepsilon = 0$). The potential of incompressible flow generated by the conformal mapping was used to start the calculation, yielding the pressure distribution displayed in Figure 3(a). The subsequent plots show the pressure distribution after completing the iteration on the fine grid and before entering the multigrid loop of each cycle. At the beginning of the 10th cycle the calculation is essentially complete. The lift and drag coefficients $CL = 0.5998$ and $CD = 0.0003$ are identical to the values obtained when this calculation was continued for 50 cycles. It appears that it should generally be possible to calculate the flows likely to be encountered in subsonic cruising flight with about 10 cycles of the multigrid alternating direction scheme.

References

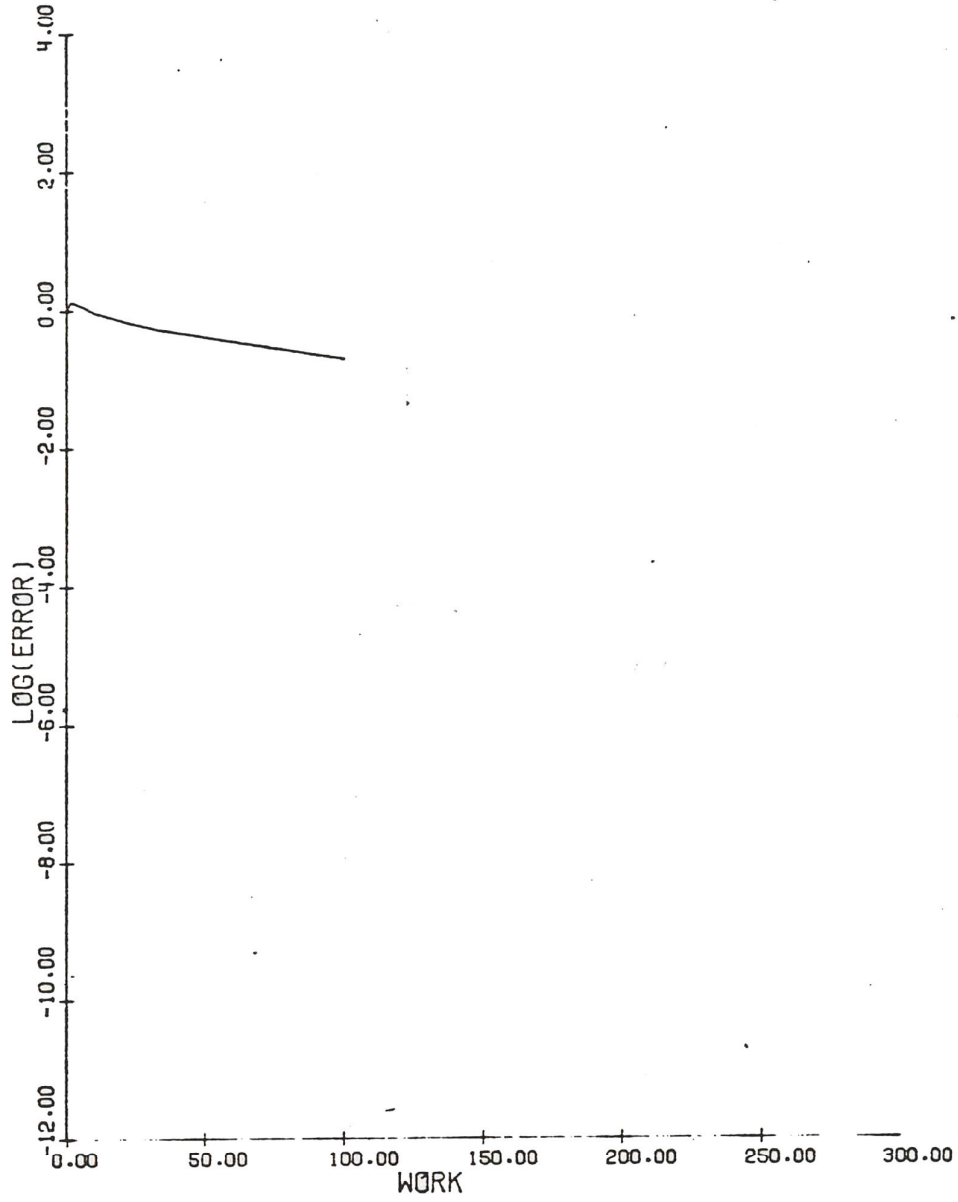
1. Federenko, R. P.: The speed of convergence of one iterative process, USSR Comp. Math. and Math. Phys., Vol. 4, 1964, pp. 227-235.
2. Bakhvalov, N. S.: On the convergence of a relaxation method with natural constraints on the elliptic operator, USSR Comp. Math. and Math Phys., Vol. 6, 1966, pp. 101-135.
3. Brandt, Achi: Multi-level adaptive solution to boundary value problems, Math. Comp., Vol. 31, 1977, pp. 333-391.
4. Nicholaides, R. A.: On the L^2 convergence of an algorithm for solving finite element systems, Math. Comp., Vol. 31, 1977, pp. 892-906.
5. Hackbusch, Wolfgang: Convergence of multi-grid iterations applied to difference equations, Koln University Mathematics Institute Report 79-5, April 1979.
6. South, J. C., and Brandt, A.: Application of a multi-level grid method to transonic flow calculation in Transonic Flow Problems machinery, edited by T. C. Ad and 14. F. Platzler, Hemisphere, Washington, 1977.
7. South, J. C., and Brandt, A.: The multi-grid method: fast relaxation for transonic flows, presentation at 13th Annual Meeting of Society of Engineering Science, Hampton, November 1976.
8. Jameson, Antony: Numerical computation of transonic flows with shock waves, Symposium Transonicum II, Gottingen, September 1975.
9. Arlinger, Bert: Multi-grid technique applied to lifting transonic flow using full potential equation, SAAB Report L-0-1 B439, December 1978.
10. Peaceman, D. W., and Rachford, H. H.: The numerical solution of parabolic and elliptic differential equations, SIAM Journal Vol. 3, 1955, pp. 28-41.
11. Jameson, Antony: Iterative solution of transonic flows over airfoils and wings, including flows at Mach 1, Comm. Pure Appl. Math., Vol. 27, 1974, pp. 283-309.

12. Murman, E. M., and Cole, J. D.: Calculation of plane steady transonic flows, AIAA Journal, Vol. 9, 1971, pp. 114-121.
13. Ballhaus, W. F., Jameson, A., and Albert, J.: Implicit approximate factorization schemes for the efficient solution of steady transonic flow problems. Third AIAA Computational Fluid Dynamics Conference, Albuquerque, June 1977.
14. Hoist, T. L., and Ballhaus, W. F.: Fast conservative schemes for the full potential equation applied to transonic flows, AIAA Journal, Vol. 17, 1979, pp. 145-152.



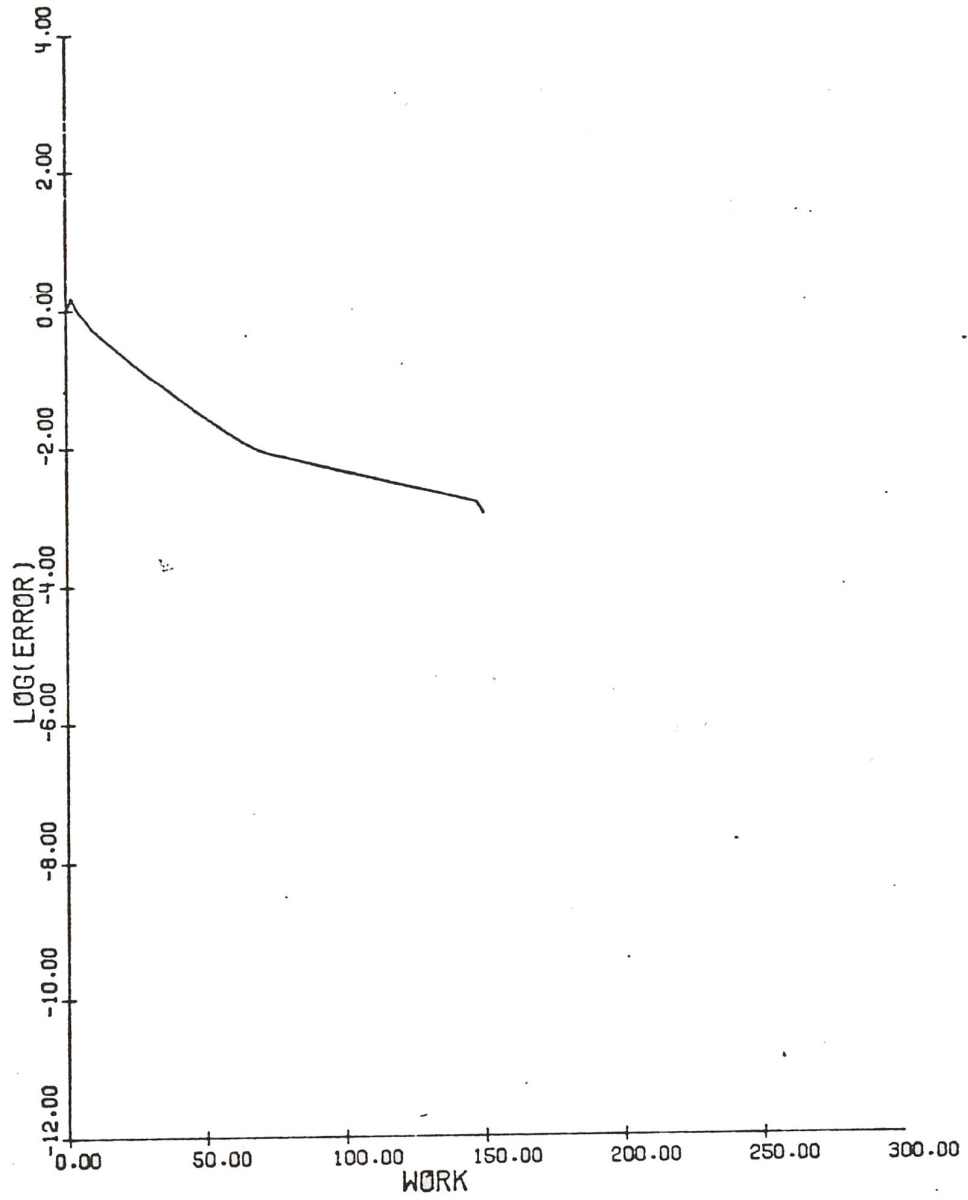
NACA 64A410
 MACH .720 ALPHA 0.000
 CL .6667 CD .0030 CM -.1478
 GRID 192X32 NCYC 29 RES .323E-12

Figure 1a. Converged pressure distribution.



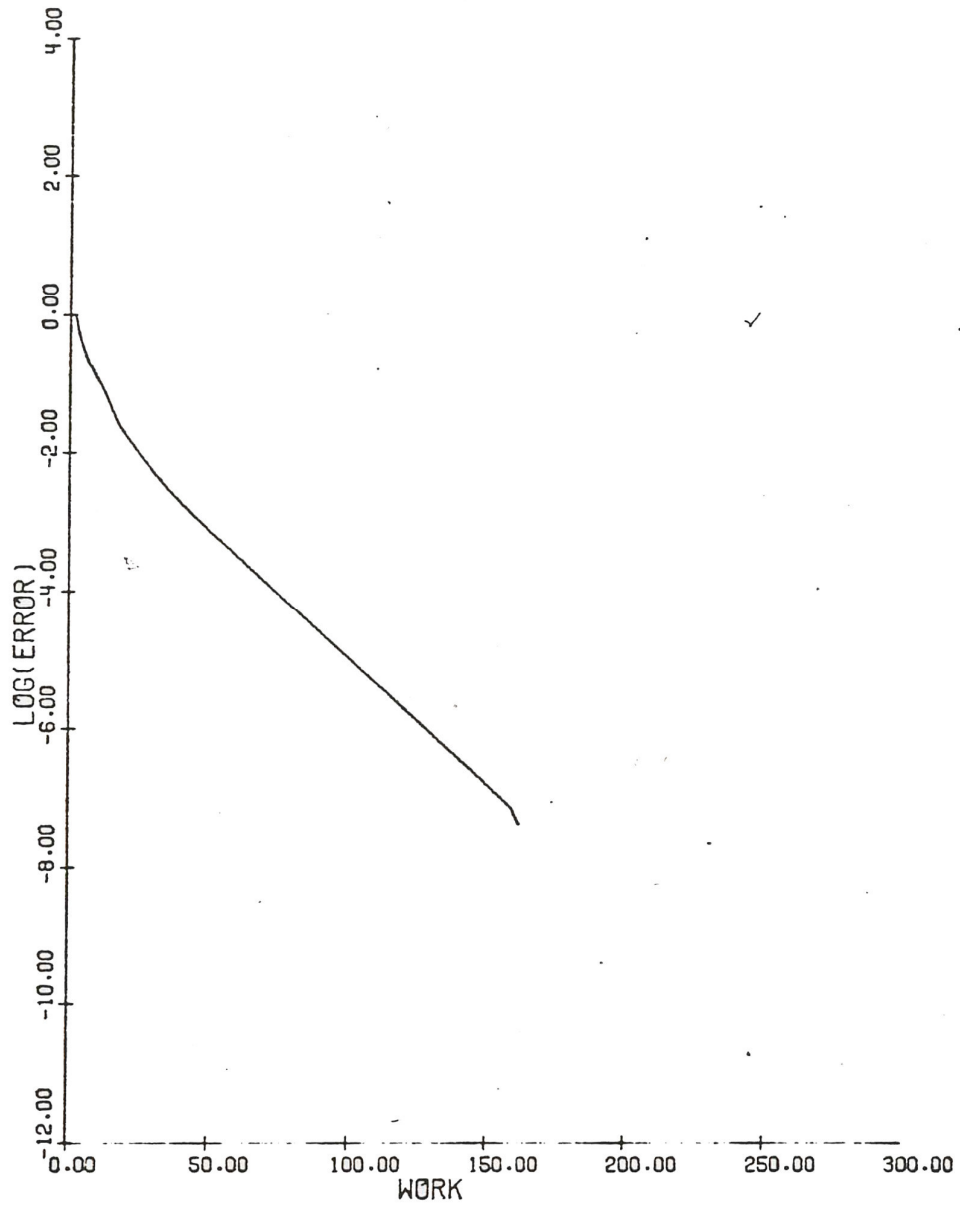
NACA 64A410			
MACH	.720	ALPHA	0.000
RESID1	.720E-04	RESID2	.144E-04
WORK	100.00	RATE	.9840
GRID	192X32		

Figure 1b. Convergence with 1 grid.



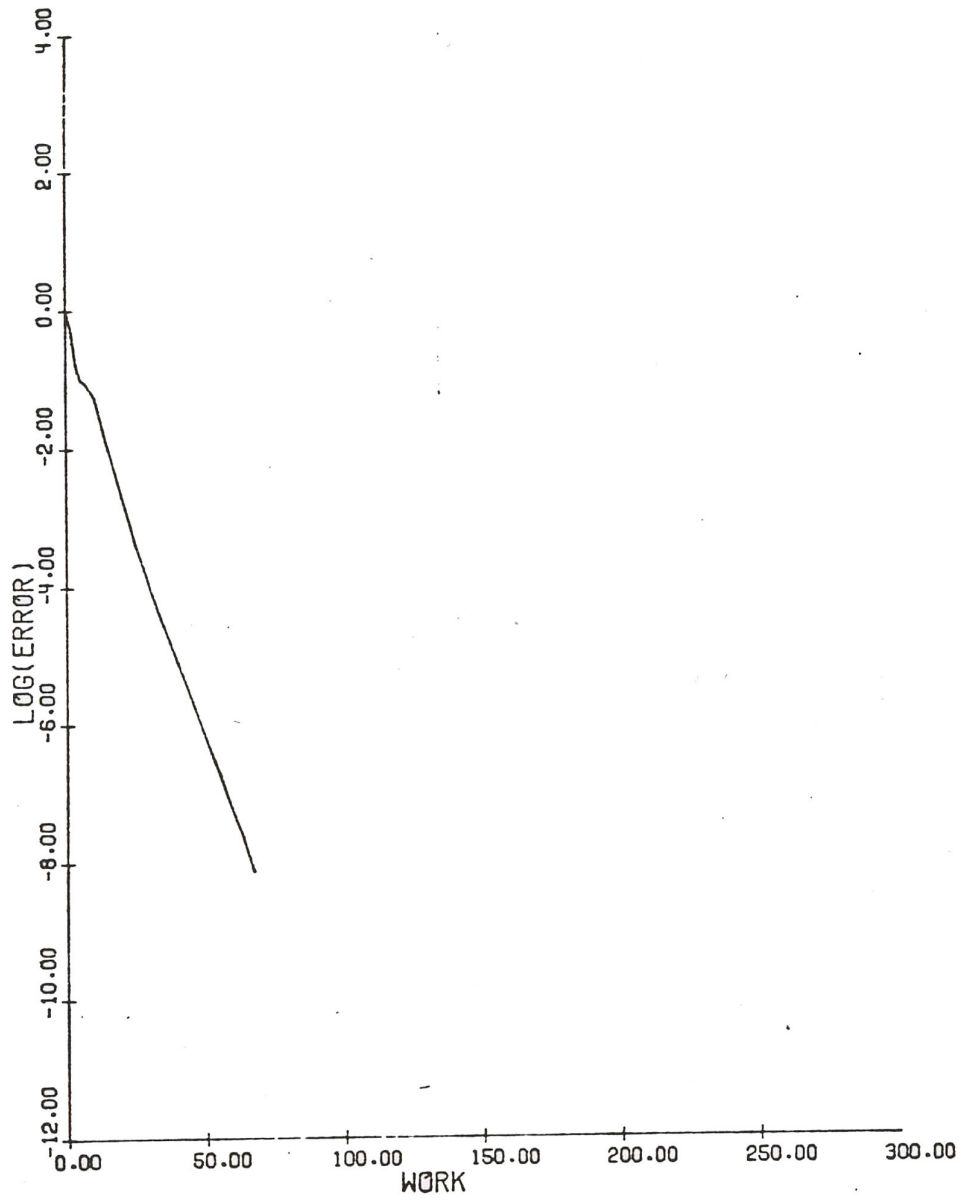
NACA 64A410			
MACH	.720	ALPHA	0.000
RESID1	.720E-04	RESID2	.780E-07
WORK	149.50	RATE	.9554
GRID	192X32		

Figure 1c. Convergence with 2 grids.



NACA 64A410			
MACH	.720	ALPHA	0.000
RESID1	.720E-04	RESID2	.308E-11
WORK	161.88	RATE	.9005
GRID	192X32		

Figure 1d. Convergence with 3 grids.

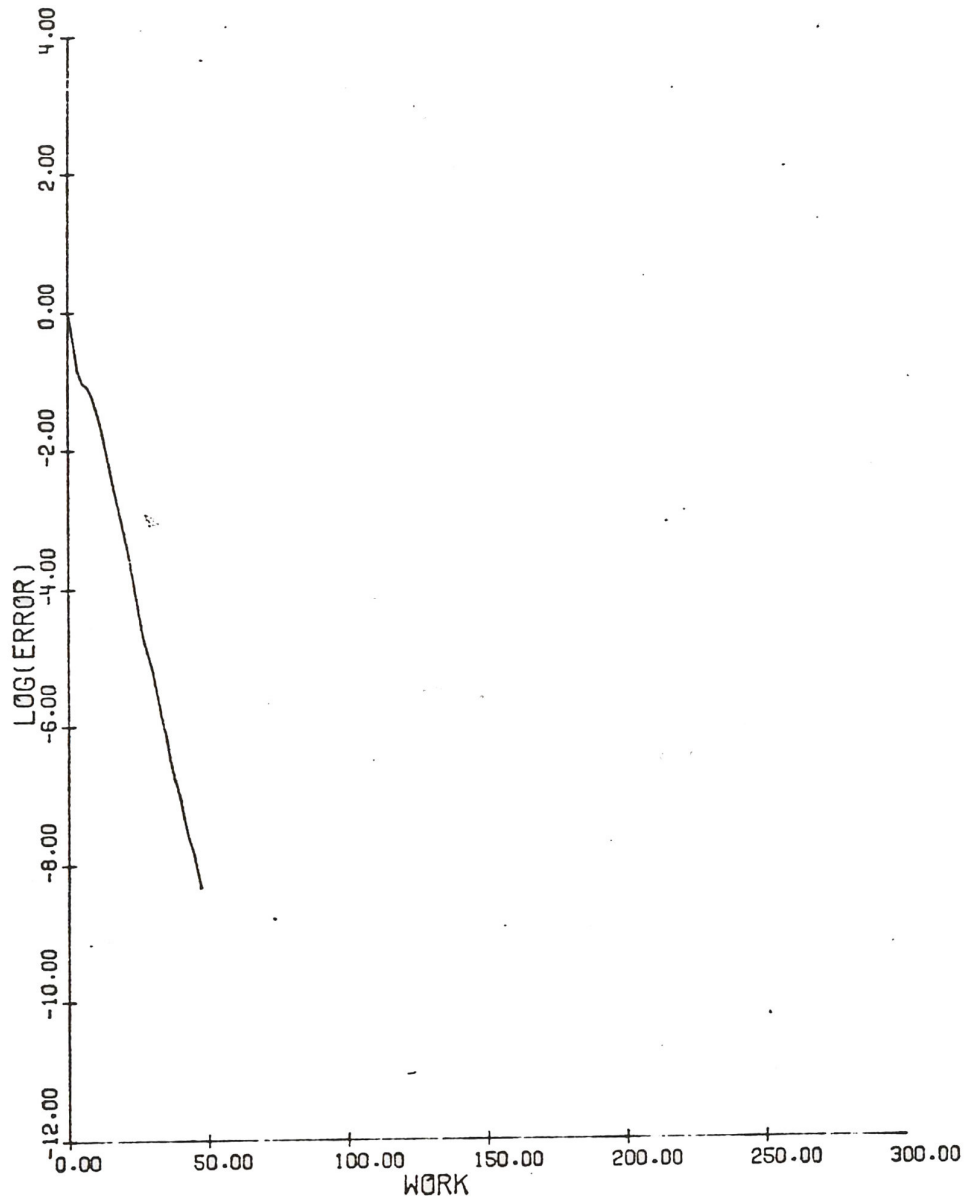


```

NACA 64A410
MACH      .720      ALPHA      0.000
RESID1    .720E-04  RESID2    .522E-12
WORK      67.25    RATE      .7568
GRID      192X32

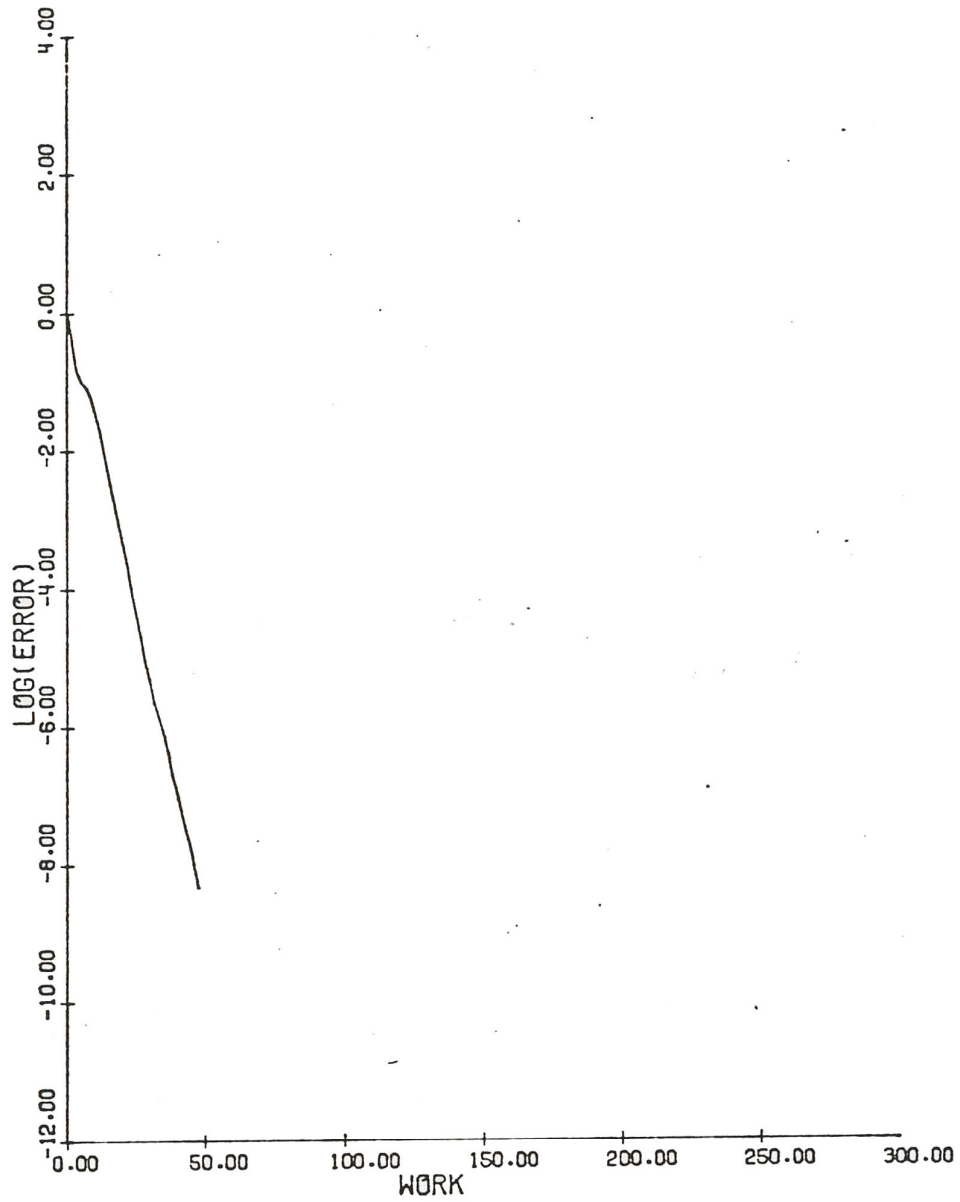
```

Figure 1e. Convergence with 4 grids.



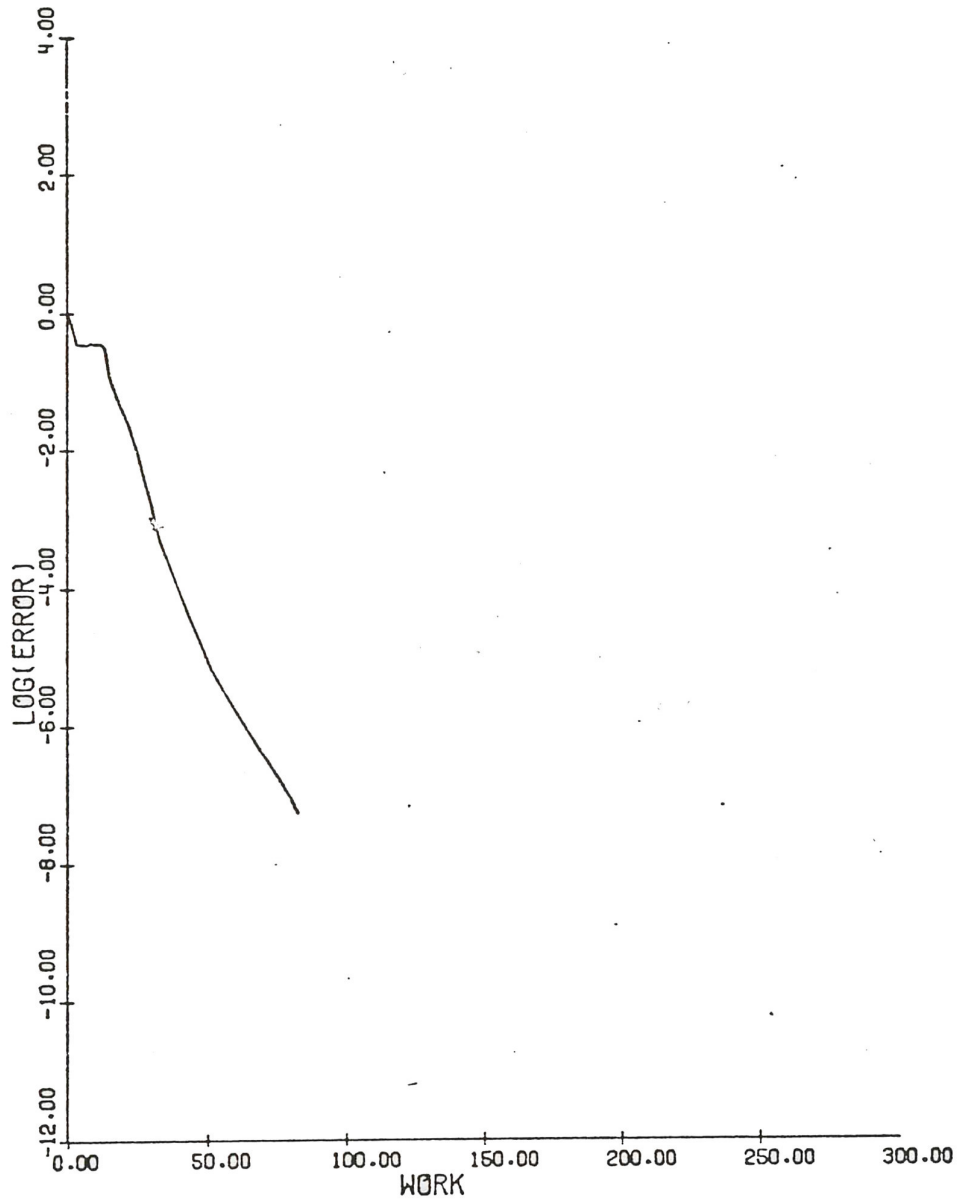
NACA 64A410			
MACH	.720	ALPHA	0.000
RESID1	.720E-04	RESID2	.323E-12
WORK	47.59	RATE	.6677
GRID	192X32		

Figure 1f. Convergence with 5 grids.



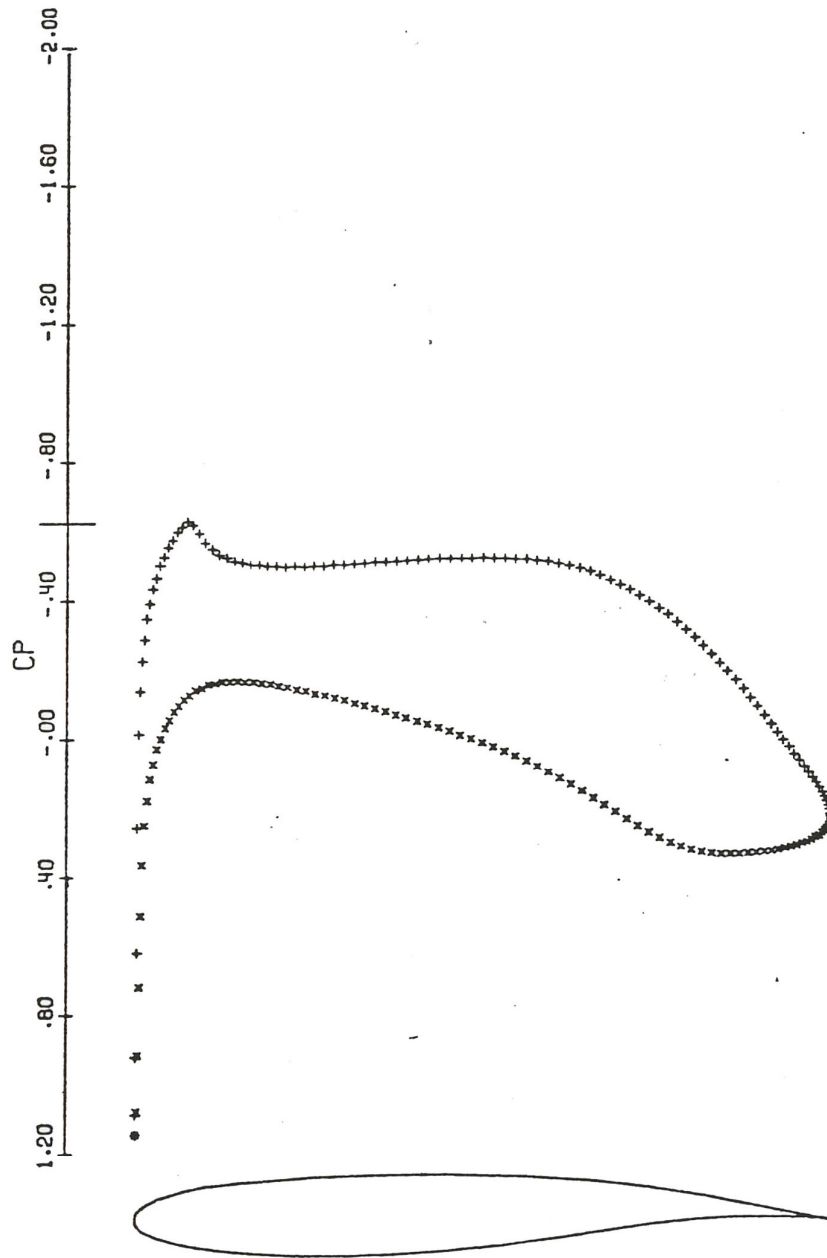
NACA 64A410			
MACH	.720	ALPHA	0.000
RESID1	.720E-04	RESID2	.341E-12
WORK	47.65	RATE	.6688
GRID	192X32		

Figure 1g. Convergence with 6 grids.



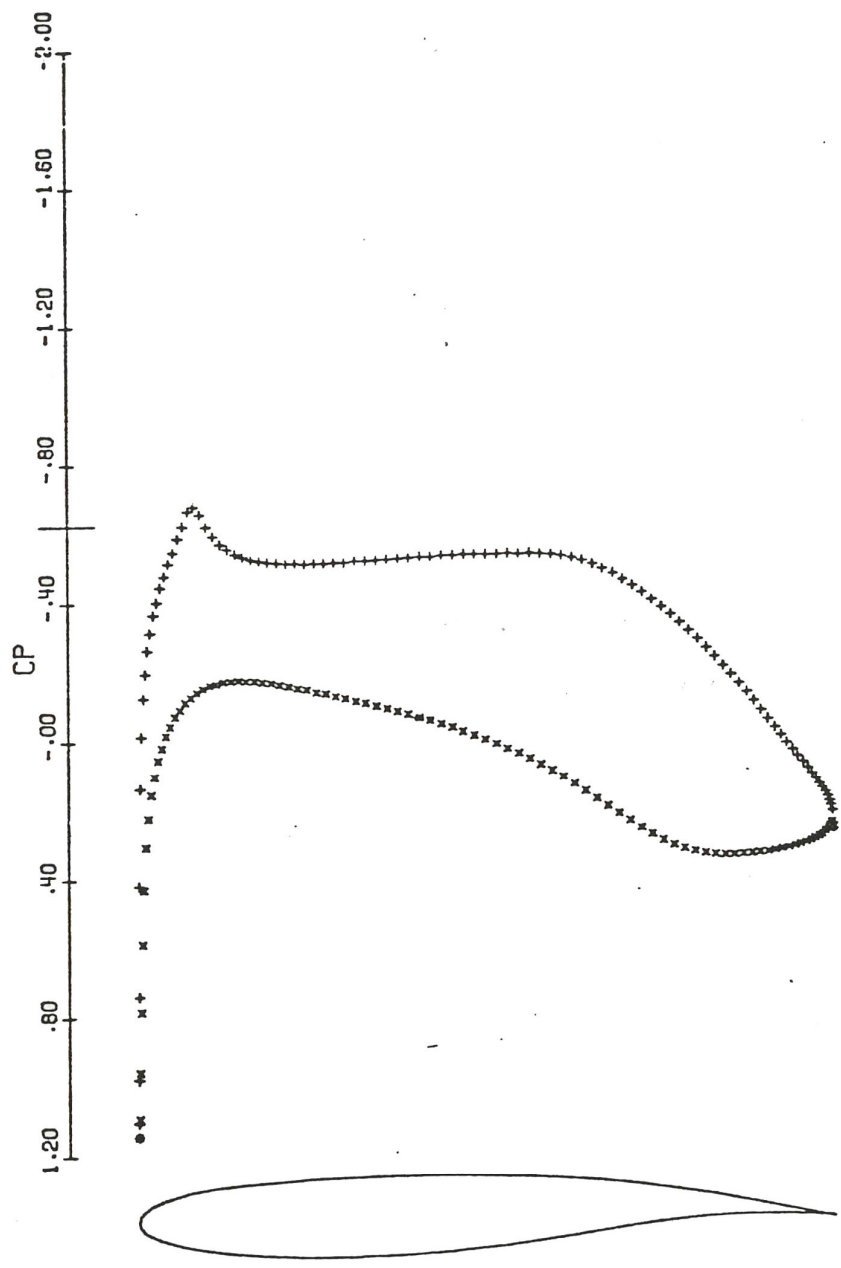
NACA 0012			
MACH	.750	ALPHA	2.000
RESID1	.916E-04	RESID2	.493E-11
WORK	82.54	RATE	.8165
GRID	192X32		

Figure 2b. Convergence with 5 grids.



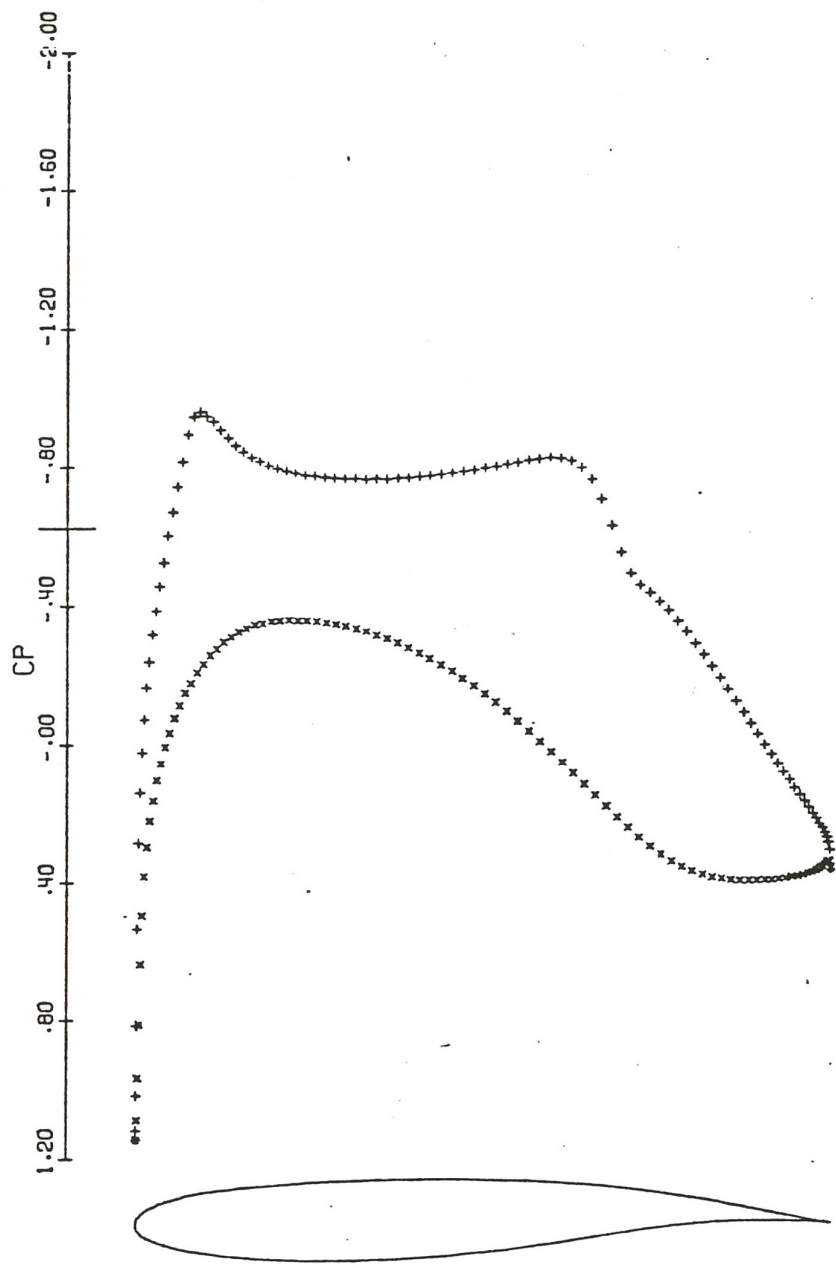
KORN AIRFOIL			
MACH	.740	ALPHA	0.000
CL	.4833	CD	.0010
GRID	192X32	NCYC	0
		CM	-.1257
		RES	.838E-04

Figure 3. Movie of Convergence



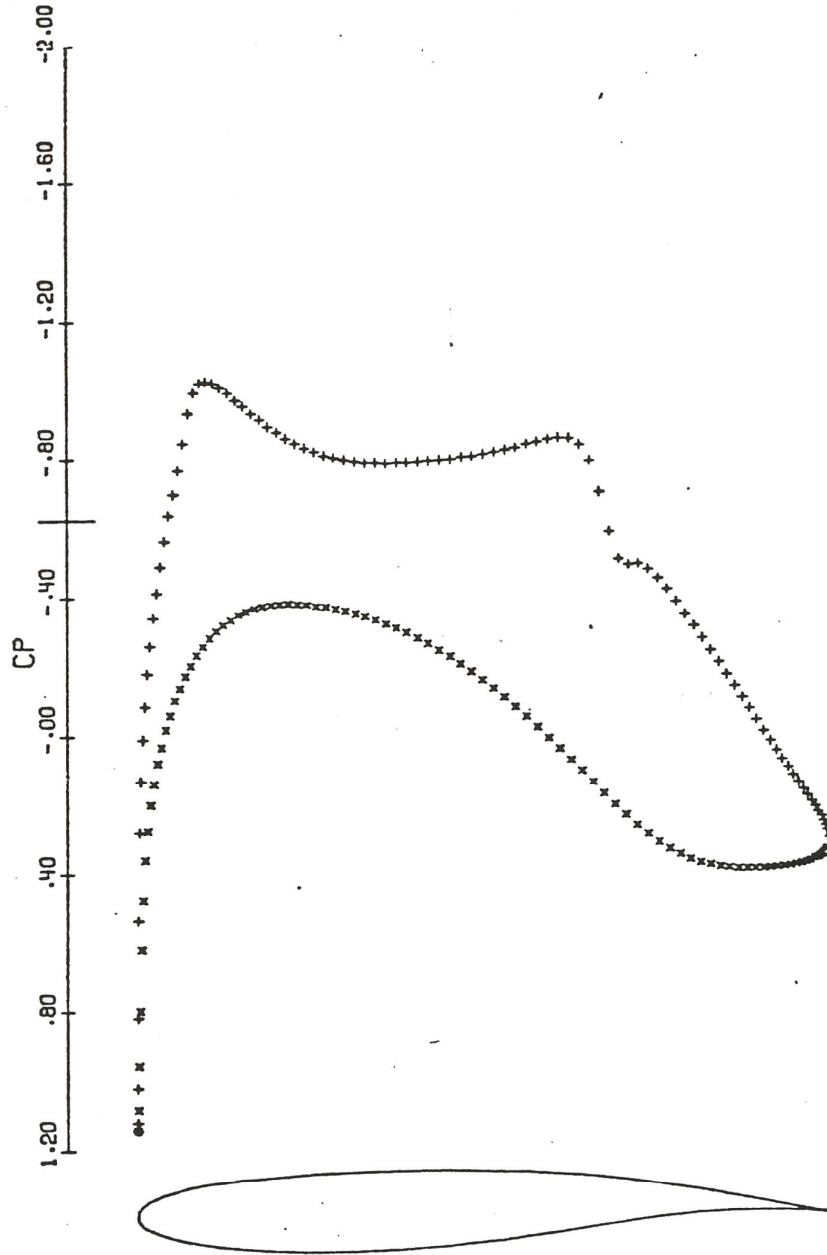
KORN AIRFOIL
 MACH .740 ALPHA 0.000
 CL .4880 CD .0041 CM -.1265
 GRID 192X32 NCYC 1 RES .107E-03

Figure 3. Continued.



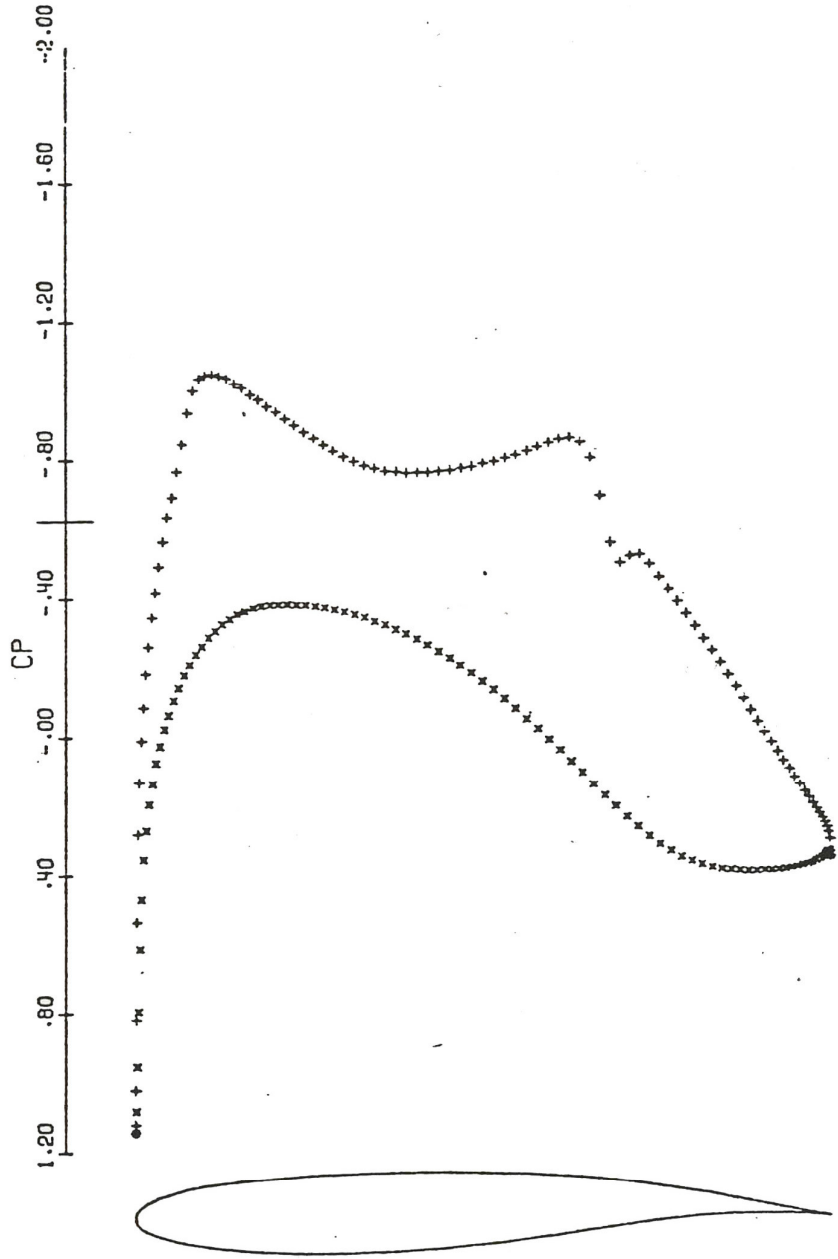
KORN AIRFOIL
 MACH .740 ALPHA 0.000
 CL .5755 CD .0033 CM -.1428
 GRID 192X32 NCYC 2 RES .283E-04

Figure 3. Continued.



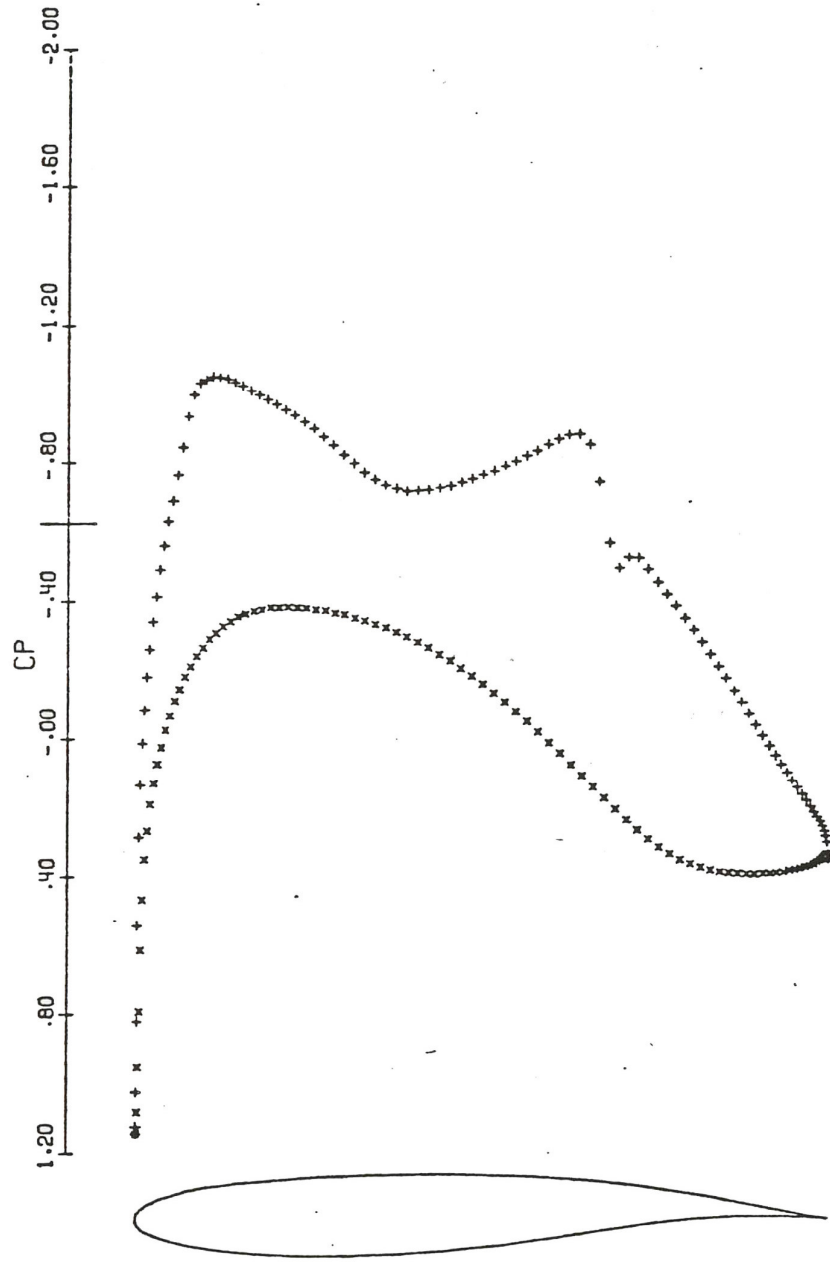
KORN AIRFOIL			
MACH	.740	ALPHA	0.000
CL	.5902	CD	.0013
GRID	192X32	NCYC	3
		CM	-.1437
		RES	.751E-05

Figure 3. Continued.



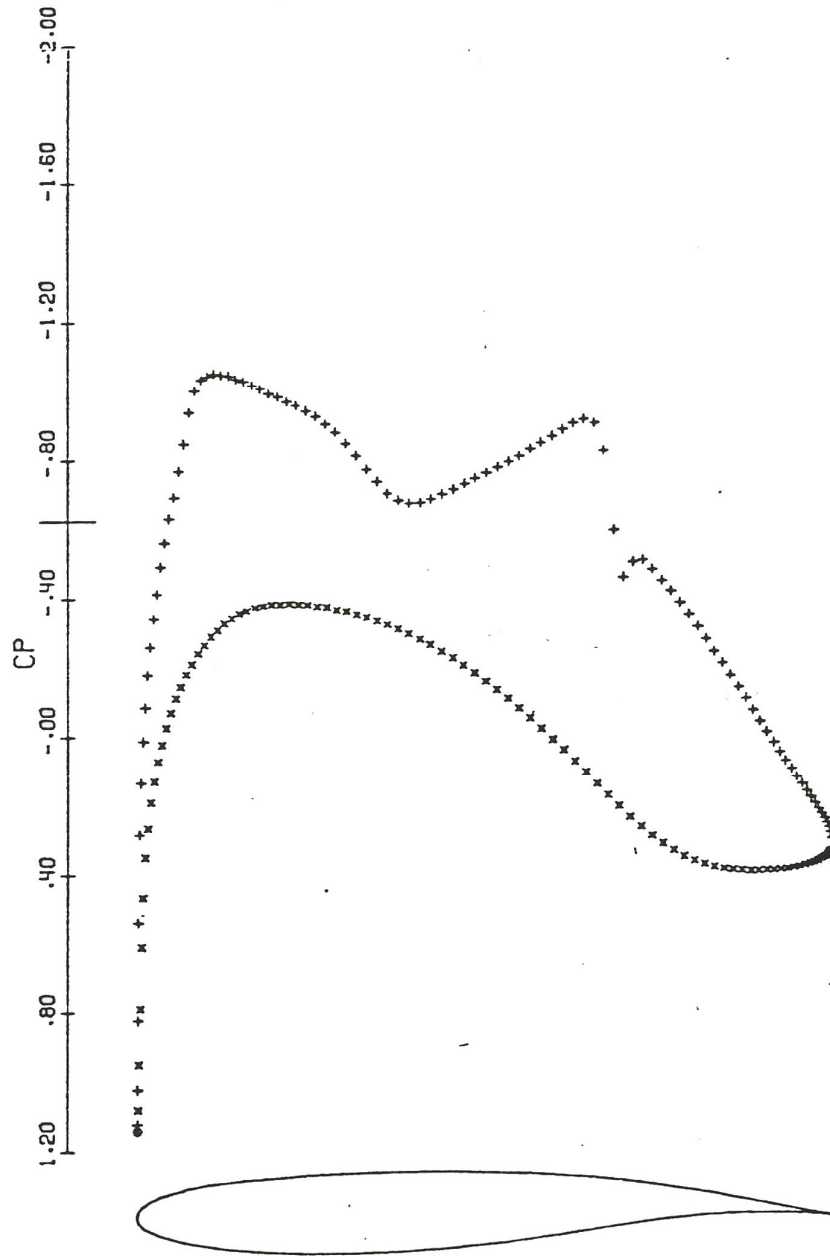
KORN AIRFOIL					
MACH	.740	ALPHA	0.000		
CL	.5950	CD	.0005	CM	-.1430
GRID	192X32	NCYC	4	RES	.440E-05

Figure 3. Continued.



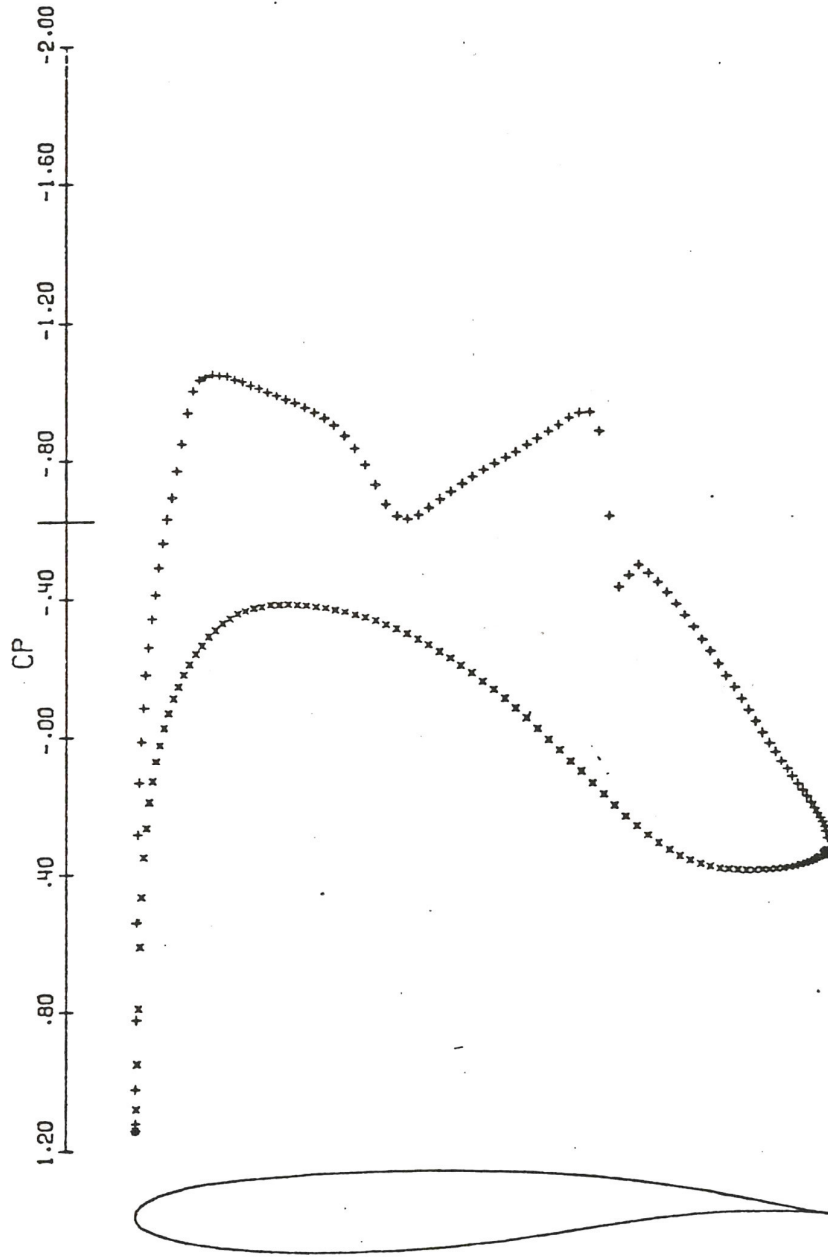
KORN AIRFOIL					
MACH	.740	ALPHA	0.000		
CL	.5953	CD	.0005	CM	-.1429
GRID	192X32	NCYC	5	RES	.364E-05

Figure 3. Continued.



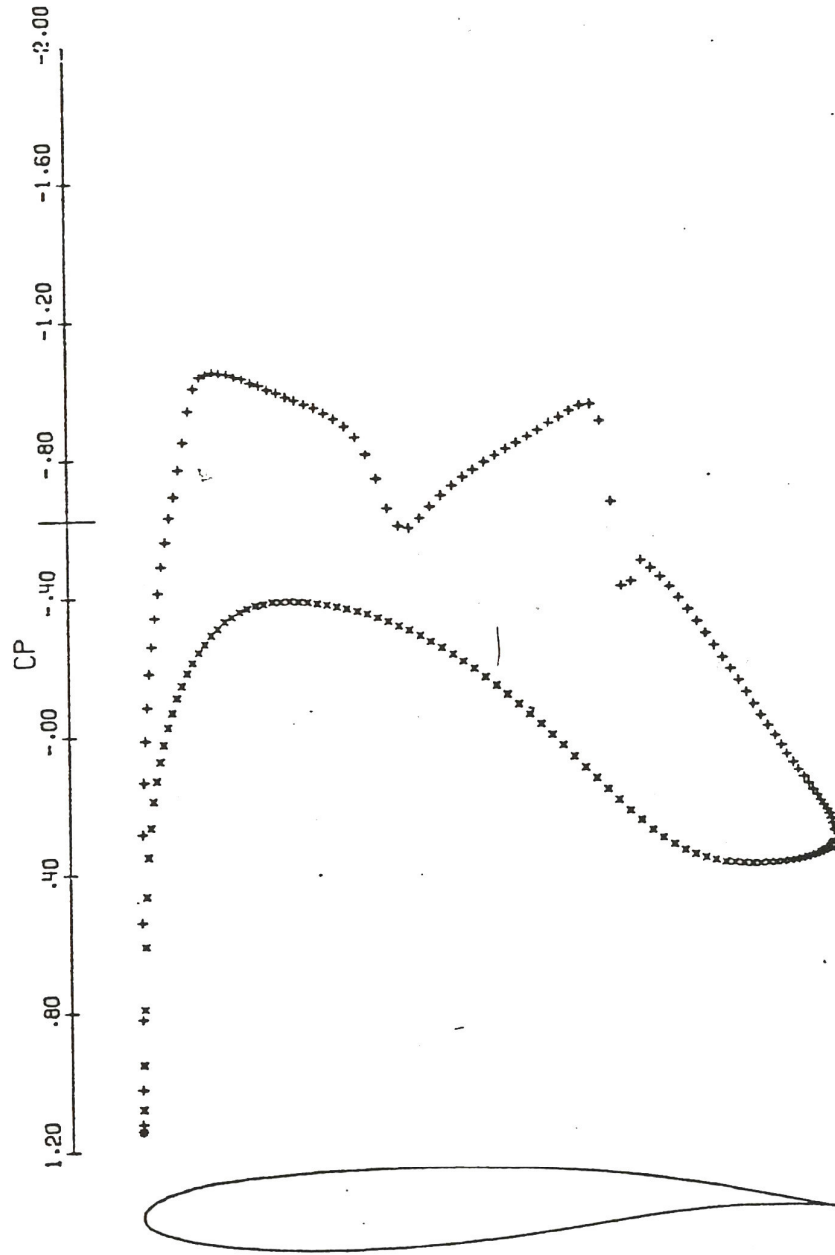
KORN AIRFOIL		
MACH	.740	ALPHA 0.000
CL	.5963	CD .0005
GRID	192X32	NCYC 6
		CM -.1431
		RES .322E-05

Figure 3. Continued.



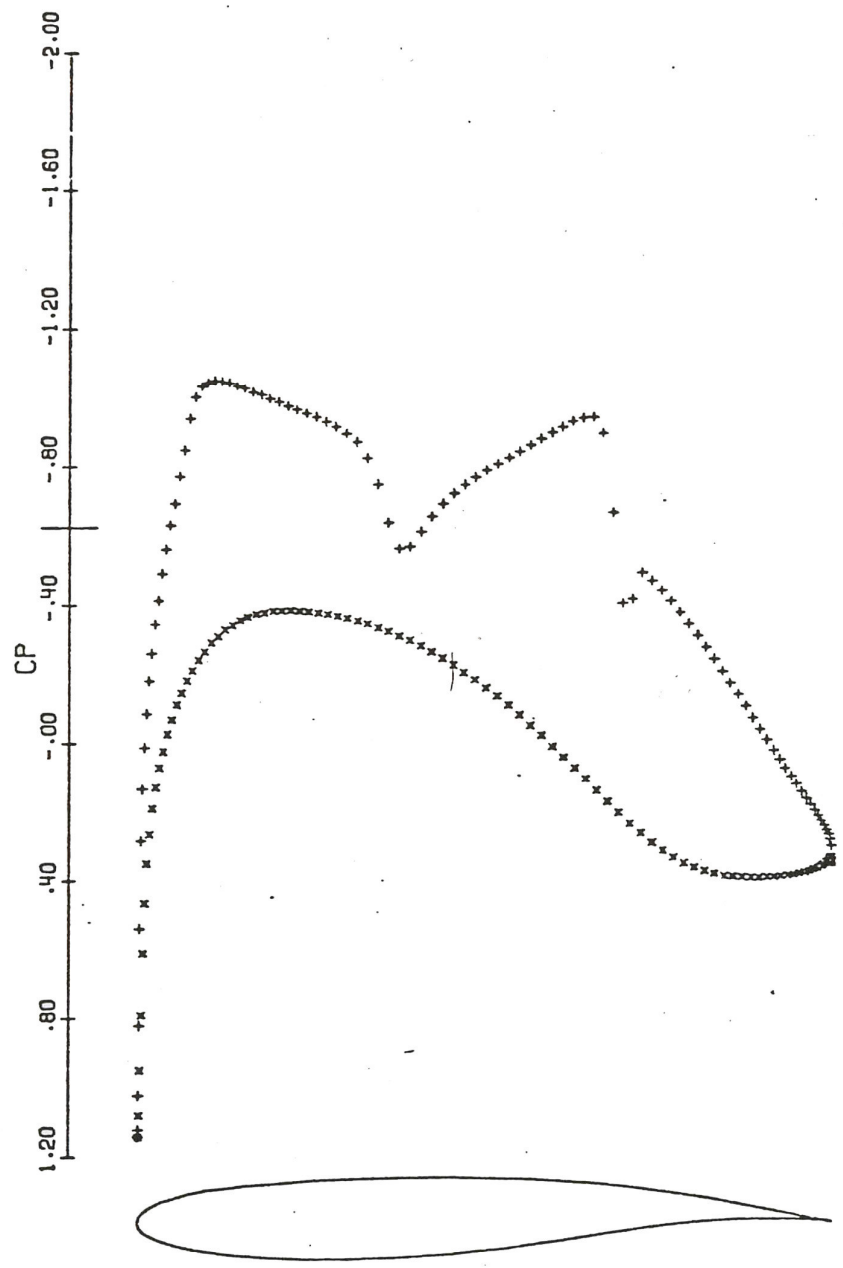
KORN AIRFOIL			
MACH	.740	ALPHA	0.000
CL	.5976	CD	.0004
GR'D	192X32	NCYC	7
		CM	-.1434
		RES	.276E-05

Figure 3. Continued.



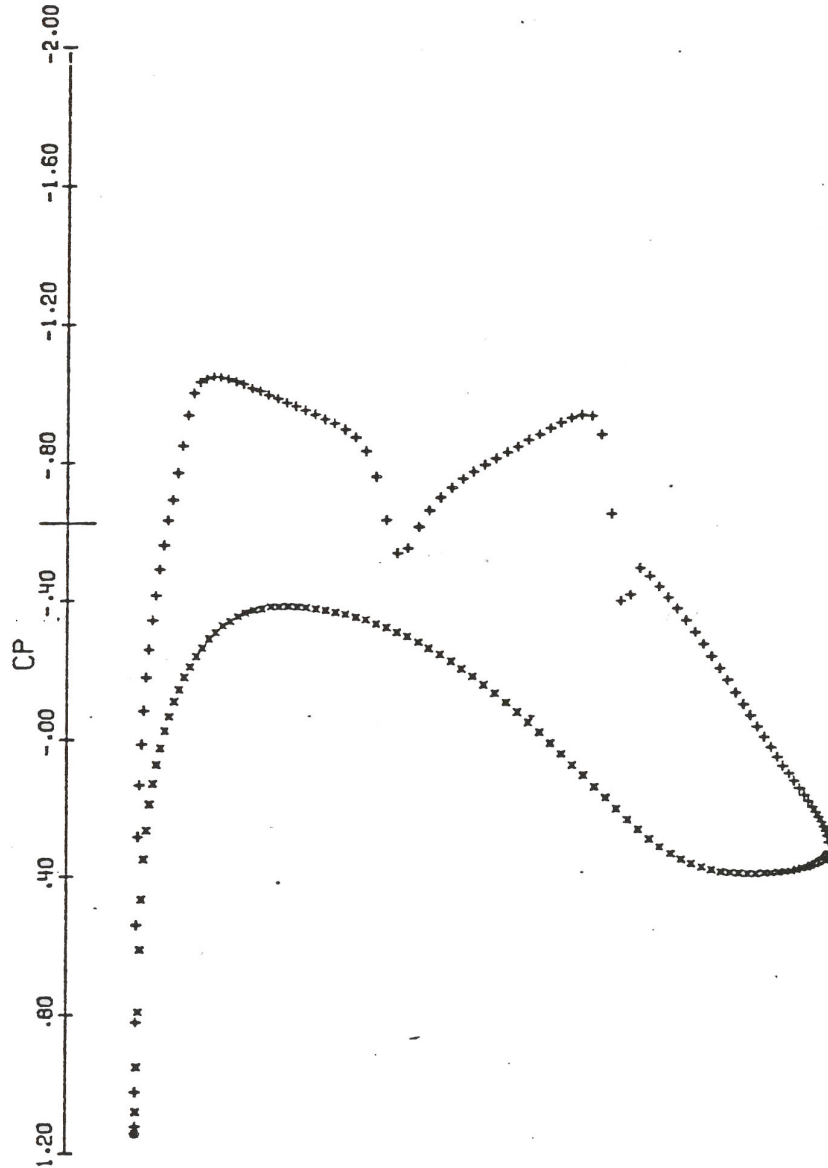
KORN AIRFOIL					
MACH	.740	ALPHA	0.000		
CL	.5988	CD	.0004	CM	-.1435
GRID	192X32	NCYC	8	RES	.207E-05

Figure 3. Continued.



KORN AIRFOIL
 MACH .740 ALPHA 0.000
 CL .5995 CD .0004 CM -.1436
 GRID 192X32 NCYC 9 RES .155E-05

Figure 3. Continued.



KORN AIRFOIL
 MACH .740 ALPHA 0.000
 CL .5998 CD .0003 CM -.1436
 GRID 192X32 NCYC 10 RES .115E-05

Figure 3. Continued.